HAL
open science

Intestinal absorption of S -nitrosothiols: permeability and transport mechanisms

Justine Bonetti, Yi Zhou, Marianne Parent, Igor Clarot, Haiyan Yu, Isabelle Fries-Raeth, Pierre Leroy, Isabelle Lartaud, Caroline Gaucher

To cite this version:

Justine Bonetti, Yi Zhou, Marianne Parent, Igor Clarot, Haiyan Yu, et al.. Intestinal absorption of S -nitrosothiols: permeability and transport mechanisms. Biochemical Pharmacology, 2018, 155, pp.21-31. 10.1016/j.bcp.2018.06.018 . hal-01824879

HAL Id: hal-01824879

https://hal.science/hal-01824879v1

Submitted on 3 Apr 2019

HAL is a multi-disciplinary open access archive for the deposit and dissemination of scientific research documents, whether they are published or not. The documents may come from teaching and research institutions in France or abroad, or from public or private research centers.

L'archive ouverte pluridisciplinaire **HAL**, est destinée au dépôt et à la diffusion de documents scientifiques de niveau recherche, publiés ou non, émanant des établissements d'enseignement et de recherche français ou étrangers, des laboratoires publics ou privés.

Biochemical Pharmacology xxx (2018) xxx-xxx

Contents lists available at ScienceDirect

Biochemical Pharmacology

journal homepage: www.elsevier.com

Intestinal absorption of *S*-nitrosothiols: Permeability and transport mechanisms

Justine Bonetti[1], Yi Zhou[1], Marianne Parent, Igor Clarot, Haiyan Yu, Isabelle Fries-Raeth, Pierre Leroy, Isabelle Lartaud, Caroline Gaucher*

Université de Lorraine, CITHEFOR, F-54000 Nancy, France

ARTICLE INFO

Keywords:
S-Nitrosothiols
Nitric oxide
Intestinal permeability
Caco-2 cells
Passive diffusion

ABSTRACT

S-Nitrosothiols, a class of NO donors, demonstrate potential benefits for cardiovascular diseases. Drugs for such chronic diseases require long term administration preferentially through the oral route. However, the absorption of *S*-nitrosothiols by the intestine, which is the first limiting barrier for their vascular bioavailability, is rarely evaluated. Using an *in vitro* model of intestinal barrier, based on human cells, the present work aimed at elucidating the mechanisms of intestinal transport (passive or active, paracellular or transcellular pathway) and at predicting the absorption site of three *S*-nitrosothiols: *S*-nitrosoglutathione (GSNO), *S*-nitroso-*N*-acetyl-*L*-cysteine (NACNO) and *S*-nitroso-*N*-acetyl-*D*-penicillamine (SNAP). These *S*-nitrosothiols include different skeletons carrying the nitroso group, which confer different physico-chemical characteristics and biological activities (antioxidant and anti-inflammatory). According to the values of apparent permeability coefficient, the three *S*-nitrosothiols belong to the medium class of permeability. The evaluation of the bidirectional apparent permeability demonstrated a passive diffusion of the three *S*-nitrosothiols. GSNO and NACNO preferentially cross the intestinal barrier though the transcellular pathway, while SNAP followed both the trans- and paracellular pathways. Finally, the permeability of NACNO was favoured at pH 6.4, which is close to the pH of the jejunal part of the intestine. Through this study, we determined the absorption mechanisms of *S*-nitrosothiols and postulated that they can be administrated through the oral route.

1. Introduction

Nitric oxide (NO) is a gaseous mediator with a short half-life (less than 5 s [1]). Due to its radical nature and oxidative activity, NO is involved in various signalling pathways among different cellular types and physiological systems. NO is continuously synthesised by oxydoreductases, *i.e.* the three endothelial, inducible or neuronal isoforms of NO synthases. The decrease in NO bioavailability, linked to vascular endothelium dysfunction and oxidative stress, plays a major role in ageing and cardiovascular chronic diseases like atherosclerosis, angina pectoris and stroke. As a result, the restoration of NO bioavailability, using among NO donors the physiologically occurring *S*-nitrosothiols, is a therapeutic key to treat cardiovascular diseases [2–7]. *S*-Nitrosothiols are formed by *S*-nitrosation – *i.e.* formation of a covalent bond between NO and a reduced thiol function of a cysteine residue belonging to high or low molecular weight proteins or peptides. *In vivo*, *S*-nitrosothiols like *S*-nitrosoalbumin, *S*-nitrosohemoglobin and *S*-nitrosoglutathione (GSNO) are the physiological forms of NO storage and transport [8]. Indeed, the formation of the *S*-NO bond extends NO half-life from 45 min up to several hours [9–10] and limits the oxidative/nitrosative stress induced by NO oxidation into peroxynitrite ions ($ONOO^-$) [11]. Despite the therapeutic potential of *S*-nitrosothiols, their half-life linked to their physico-chemical instability (heat, light, metallic cations,…) and/or enzymatic (redoxines or, for GSNO only, γ-glutamyltransferase) degradation, is too short for chronic diseases treatment [12].

Nowadays, many preclinical studies focused on cardiovascular therapeutics using *S*-nitrosothiols [6,13–17]. For example, daily intraperitoneal administration of *S*-nitroso-*N*-acetyl-*L*-cysteine (NACNO) for two weeks shows anti-atherosclerotic effects in mice [13]. However, compared to the oral route, the intraperitoneal administration is less suitable for chronic treatments. GSNO administration through the oral route in a context of stroke [14] results in neuroprotective effects: GSNO maintains the blood-brain barrier in-

* Corresponding author at: Université de Lorraine, CITHEFOR EA 3452, Faculté de Pharmacie, BP 80403, F-54001 Nancy Cedex, France.
Email address: caroline.gaucher@univ-lorraine.fr (C. Gaucher)

[1] Both authors contributed equally to this work.

https://doi.org/10.1016/j.bcp.2018.06.018
Received 12 April 2018; Accepted 19 June 2018
Available online xxx
0006-2952/ © 2018.

UNCORRECTED PROOF

tegrity, reduces peroxynitrite formation and stabilises several deleterious factors *via S*-nitrosation [13–16]. Despite such beneficial effects following oral administration, to the best of our knowledge, no study evaluated the mechanisms of intestinal absorption of GSNO and other *S*-nitrosothiols. Only Pinheiro et al. [17] demonstrated that oral administration of nitrite and nitrate ions (stable NO derived species) to rats increased the concentration of circulating *S*-nitrosothiols, thus produced antihypertensive effects. This study indirectly proves the intestinal absorption of *S*-nitrosothiols without elucidated the underlying mechanisms. However, the understanding of the intestinal absorption mechanisms of *S*-nitrosothiols is a prerequisite to control the dose and the kinetic of NO reaching its action sites.

To predict the intestinal absorption of drugs, the Biopharmaceutical Classification System (BCS) [18] defines four classes based on the physico-chemical properties (solubility) and intestinal permeability of drugs. The intestinal permeability of a drug is characterised, using *in vitro* or *ex vivo* models, by apparent permeability coefficient (Papp) from low permeability ($<1\times10^{-6}$ cm.s^{-1}) to high permeability ($\geq10\times10^{-6}$ cm.s^{-1}) including also a medium permeability class [19]. Thus far, only one of our studies was interested in the improvement and the prolongation of GSNO intestinal absorption by proposing alginate/chitosan nanocomposite formulation [20]. Using an *in vitro* intestinal barrier model of differentiated Caco-2 cells, we showed low intestinal permeability for GSNO with a Papp of 0.83×10^{-7} cm.s^{-1}. The nanocomposite formulation delayed GSNO absorption up to 24 h (1 h for free GSNO) and multiplied by four the Papp value (3.41×10^{-7} cm.s^{-1}) even if GSNO stayed in the low class of permeability [20]. This study showed the ability for GSNO to cross the intestinal barrier model and the possibility to modulate its kinetics of absorption. This opens new therapeutic applications in the treatment of chronic pathologies linked to a decrease of NO bioavailability.

Intestinal absorption of low molecular weight molecules is mainly driven by their physico-chemical properties such as lipophilicity, correlated with the octanol/water partition coefficient, expressed as a logarithmic value (log P), and the ionisation constant (pKa). For *S*-nitrosothiols, the log P value is driven by the skeleton carrying NO. GSNO, NACNO and *S*-nitroso-*N*-acetyl-*D*-penicillamine (SNAP), the three main *S*-nitrosothiols described in the literature, are characterised by calculated log P value of −2.70, −0.47 and 1.08, respectively [2]. The skeleton carrying NO presents also different therapeutic properties linked with its chemical structure. GSNO is a physiological *S*-nitrosothiol [21], present in the cytosol at a high concentration especially in erythrocytes [22], platelets and cerebral tissue. Its reduced glutathione (GSH) skeleton shows an antioxidant chemical structure thanks to its thiol functional group and forms, with the glutathione disulphide (GSSG), the intracellular redox buffer. NACNO and SNAP are synthetic *S*-nitrosothiols. NACNO with its *N*-acetyl-*L*-cysteine (NAC) skeleton possesses also an antioxidant activity in accordance with its chemical structure (thiol function). Furthermore, NAC is already used in human medicine as a mucolytic agent (oral administration) or as the antidote in acetaminophen intoxication [23]. SNAP shows in addition to its antioxidant properties (thiol function), an anti-inflammatory skeleton, *N*-acetyl-*D*-penicillamine (NAP) is used in the treatment of Wilson's disease (Trolovol®) and rheumatoid arthritis.

In this study, using an *in vitro* cell model of intestinal barrier, we propose to elucidate the intestinal transport mechanisms of *S*-nitrosothiols and NO in relation to their physico-chemical properties. Three different conditions were studied, i) permeability from the apical to the basolateral compartment, ii) permeability from the basolateral to the apical compartment to highlight an active transport such as drug influx/efflux, or a passive diffusion, and iii) permeability from an acidified apical compartment, mimicking the luminal intestinal pH of the jejunum, the major site of amino acid absorption [24].

2. Material and methods

2.1. Material and reagents

Eagle's Minimum Essential Medium (EMEM), foetal bovine serum (FBS), sodium pyruvate, penicillin 10 000 U.mL^{-1} and streptomycin 10 mg.mL^{-1} mix, trypsin, non-essential amino acids, glutamine, Hank's Balanced Salt Solution (HBSS Ca^{2+}/Mg^{2+}), sodium nitrate ($NaNO_3$), 2,3-diaminonaphthalene (DAN), 1.0 M hydrochloric acid (HCl) solution, propranolol hydrochloride, furosemide salt, triethylamine, 2-(*N*-morpholino)ethanesulfonic acid (MES), Trisma base (Tris), sodium chloride (NaCl), Igepal CA-630, sodium dodecyl sulfate (SDS), ethylenediaminetetraacetic acid (EDTA), neocuproine and *N*-ethylmaleimide (NEM) were purchased from Sigma, France. Mercuric chloride ($HgCl_2$), orthophosphoric acid and sodium tetraborate were purchased from Prolabo (VWR). Sodium nitrite ($NaNO_2$) from Merck, sodium hydroxide (NaOH) from VWR Chemicals, methanol from Carlo Erba Reagents and acetonitrile was from Biosolve. Nitrite/nitrate fluorimetric kit was purchased from Cayman Chemical (Ref. 780051).

2.2. S-Nitrosothiols synthesis

GSNO, NACNO and SNAP were synthesised according to a previously described method [25]. Briefly, GSH, NAC or NAP were incubated with one equivalent of sodium nitrite under acidic condition. Then, the pH was shifted to 7.4 using a phosphate buffered saline (PBS 0.148 M) solution. The final concentration was assessed by UV–Vis. spectrophotometry (Shimadzu; UV-spectrophotometer; UV-1800) using the specific molar absorbance of the *S*-NO bond at 334 nm for GSNO and NACNO ($\varepsilon_{GSNO} = 922\,M^{-1}\,cm^{-1}$; $\varepsilon_{NACNO} = 900\,M^{-1}\,cm^{-1}$) and at 340 nm for SNAP ($\varepsilon_{SNAP} = 1020\,M^{-1}\,cm^{-1}$).

2.3. Caco-2 cells culture and cytocompatibility

Intestinal Caco-2 cells (ATCC® HTB-37™) from passage 36 to 45 were grown in complete medium consisting of EMEM supplemented with 10% (v/v) of FBS, 4 mM of glutamine, 100 U/mL of penicillin, 100 U/mL of streptomycin, 1% (v/v) of non-essential amino acids. Cells were cultivated at 37 °C under 5% CO_2 (v/v) in a humidified incubator. Caco-2 cells were seeded in 96-wells plates at 2×10^4 cells/well 24 h before experiment. They were then exposed to each *S*-nitrosothiol (from 10 to 100 μM) for 24 h at 37 °C, complete medium being used as control. Cytocompatibility was assessed through metabolic activity with the 3(4,5-dimethylthiazol-2-yl)-2,5-diphenyltetrazolium bromide (MTT) assay. The absorbance of extracted formazan crystals was read at 570 nm with a reference at 630 nm (EL 800 microplate reader, Bio-TEK Instrument, Inc®, France). Metabolic activity in control condition was considered as 100%.

2.4. Intestinal permeability of reference molecules and S-nitrosothiols

Caco-2 cells were seeded at 2×10^6 cell/cm^2 on cell culture inserts (Transwell®, Corning, USA, membrane with 0.4 μm pore size, 1.12 cm^2 area or 4.97 cm^2) disposed in a 12-wells or 6-wells plate, respectively. The complete medium was replaced every two days during the first week of cell proliferation. During the second week, the medium was replaced every day until the differentiated cell mono-

UNCORRECTED PROOF

layer was formed (14–15 days). The formation of the barrier was followed by transepithelial electrical resistance (TEER) measurement using a Millicell®-Electrical Resistance system (Millipore, USA) and validated for TEER values higher than 500 Ω.cm^2.

The bidirectional permeability of each *S*-nitrosothiol across the Caco-2 monolayer was evaluated from the apical to basolateral (A-B) compartment, mimicking physiological permeability conditions (intestinal lumen to blood compartment), and from the basolateral to the apical (B-A) (Fig. 1) compartment in HBSS at pH 7.4 to evaluate possible efflux mechanisms. A third condition evaluates the importance of the influence of luminal pH adjusted to 6.4 with 0.5 M MES solution in the apical compartment to determine the intestinal site of absorption (intestinal segment).

The concentration of *S*-nitrosothiols used to study the permeability in each direction was the same (100 μM). Since the apical and the basolateral compartments have different volumes (0.5 and 1.5 mL, respectively), the initial amounts of *S*-nitrosothiol for A-B and for B-A permeability studies were 50 and 150 nmol, respectively. $NaNO_2$ treatment (100 μM) was used as a positive control for nitrite ions permeability. The bidirectional permeability of propranolol (50 μM) and furosemide (100 μM), two reference molecules belonging to the high and low permeability class, respectively, was also assessed to surround the permeability of *S*-nitrosothiols [26,27] and to validate our model faced to the literature.

Permeability tests were conducted during 4 h under orbital shaking (500 rpm) at 37 °C. In the acceptor compartment, *S*-nitrosothiols were considered as RSNO because the R skeleton carrying NO cannot be identified by the methodology of quantification used. Reference molecules as well as NOx species (RSNO, nitrite ions and nitrate ions) were quantified after 1 h (entire volume of acceptor compartment removed) in the acceptor compartment and after 4 h in both compartments (for methodologies, see Sections 2.5. and 2.6.). RSNO and nitrite ions were also quantified inside the cells after 1 h and 4 h of permeability study.

At the end of the study, the integrity of the intestinal cell monolayer was checked by measuring the TEER value and the permeability of sodium fluorescein (5 μM), a marker of low paracellular permeability. A TEER value higher than 300 Ω.cm^2 as well as a 5% of fluorescein permeability validated the integrity of the intestinal monolayer at the end of the experiment [28,29].

2.5. Quantification of S-nitrosothiols, nitrite and nitrate ions

S-Nitrosothiols and nitrite ions were immediately quantified using a fluorimetric method [30] with standard curves of GSNO and sodium nitrite, respectively (Table 1). Briefly, N_2O_3 generated from acidified nitrite ions reacts with DAN in the presence (for RSNO) or absence (for nitrite ions) of $HgCl_2$ producing 2,3-naphthotriazole that emits fluorescence at 415 nm after excitation at 375 nm (JASCO FP-8300, France). Nitrate ions quantification, using a standard curve of sodium nitrate included a reduction step to nitrite ions by reacting with nitrate reductase and its cofactors before the addition of DAN reagent (fluorimetric kit nitrite/nitrate Cayman Chemical) (Table 1). The concentration of nitrite ions (DAN assay) was subtracted from the value obtained by DAN-Hg^{2+} quantification to obtain the RSNO concentration and from the nitrate reductase quantification to obtain the nitrate ions concentration. The cumulative amounts of RSNO, NO_2^- and NO_3^- crossing the Caco-2 monolayer were calculated from the concentrations measured at 1 h and 4 h of the permeability studies in the acceptor compartment.

For intracellular quantifications, cells were lysed in 50 mM Tris buffer pH 6.8 added with 150 mM of NaCl, 1% of Igepal CA-630 (v/v), 0.1% of SDS (v/v), 1 mM of EDTA, 0.1 mM of neocuproine, 20 mM of sodium tetraborate and 10 mM of NEM.

2.6. Quantification of furosemide and propranolol

This procedure was adapted from [31–33] for propranolol and from [34] for furosemide. Briefly, the separation was performed on a C18 analytical column (Macherey-Nagel LiChrospher RP 18e; 5 μm; 125 × 4 mm) eluted with a mobile phase composed of acetonitrile added with 14 mM triethylamine in water buffered with orthophosphoric acid, pH 2.5 (30/70; v/v) at a flow rate of 1.0 mL.min^{-1} and with a column temperature of 40 °C. The injection volume was 20 μL. Propranolol and furosemide were detected using a spectrofluorometric detector (model Jasco FP-920) set at $\lambda_{ex} = 230$ nm/$\lambda_{em} = 340$ nm, and $\lambda_{ex} = 235$ nm/$\lambda_{em} = 402$ nm, respectively. Standard curves of propranolol and furosemide were established between 0.5 and 10.0 μM and 62.5 nM to 2.0 μM, respectively.

2.7. Calculation of apparent permeability coefficients and recovery rates

2.7.1. Apparent permeability coefficient

The apparent permeability coefficient (Papp) values were calculated using the following equation (Eq. (1):

$$Papp = \frac{dQ}{dt} \times \frac{1}{A \times C_0} \quad (1)$$

dQ/dt (mol.s^{-1}) refers to the permeability rate of reference molecules, RSNO or NOx species (mol) in the acceptor compartment at the time (s) of quantification, A (cm^2) refers to membrane diffusion area, and C_0 (mol.mL-1 or mol.cm^{-3}) refers to the initial concentration in the donor compartment.

2.7.2. Recovery rate

Mass balance was calculated as the addition of the amount of drug recovered in the acceptor compartment after each interval and in the donor compartment at the end of the experiment.

2.8. Statistical analysis

Results are shown as mean ± standard deviation (SD), based on 3 or 4 independent experiments in duplicate. Values were compared with one-way ANOVA (treatments) or two-way ANOVA (treatment

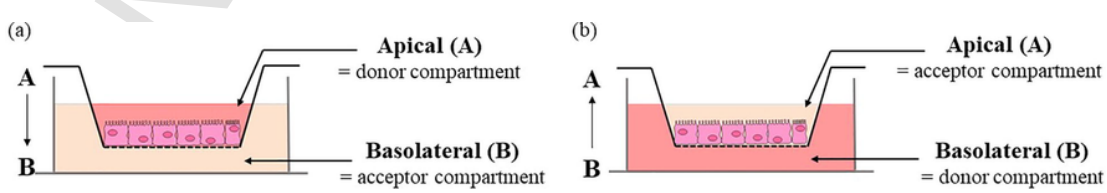

Fig. 1. Schematic representation of the bidirectional permeability of *S*-nitrosothiols across the Caco-2 monolayer. (a) From the apical (intestinal lumen) to the basolateral (bloodstream) compartment (on the left, A → B) to study physiological intestinal permeability, (b) from the basolateral to the apical compartment (on the right, B → A) to study S-nitrosothiol efflux.

UNCORRECTED PROOF

Table 1
Standard curves validation parameters for *S*-nitrosothiols (RSNO), nitrite ions (NO_2^-) and nitrate ions (NO_3^-) in HBSS with Ca^{2+}/Mg^{2+}. Mean ± SD; n = 3.

	Concentration range (μM)	Standard curves equation	Relative standard deviation (%)
RSNO	0.1–2.0	y = (1451 ± 236)x + (399 ± 98)	0.1 μM: 12.3 2 μM: 1.2
NO_2^-	2 μM: 3.2	y = (1527 ± 96)x + (435 ± 89)	0.1 μM: 4.3
NO_3^-	0.01–3.75	y = (264 ± 22)x + (1719 ± 116)	0.01 μM: 8.4 3.75 μM: 5.1

and time) followed by a Bonferroni's post-test using the Graphpad Prism 5 software; $p < 0.05$ was considered as statistically significant. Statistics are analysed excluding $NaNO_2$ treatments, which too high permeability values interfered with the statistical comparison of *S*-nitrosothiols.

3. Results

3.1. Cytocompatibility

Cell viability was not affected by any of the *S*-nitrosothiols presently tested and $NaNO_2$, with more 80% of viability independently of the concentration used (Fig. 2). For all the forthcoming experiments, a concentration of 100 μM of each *S*-nitrosothiol will be safely used.

3.2. S-Nitrosothiols permeability from the apical to the basolateral compartment

S-Nitrosothiols permeation through the intestinal barrier model, evaluated in the A-B direction, showed the same profile for each treatment (GSNO, NACNO and SNAP) (Fig. 3). Each *S*-nitrosothiol (treatment) was permeated under three different chemical species. The RSNO form (Fig. 3A) was less permeated (0.50% ± 0.14% of the initial amount deposited in the donor compartment) than the NO_2^- (the first stable oxidation degree of NO in aqueous media) and NO_3^- ionic forms (4.8% ± 1.9% and 7.9% ± 2.4% of the initial amount, respectively). The NACNO treatment led to a higher permeation under the RSNO form than the GSNO and SNAP treatments (Fig. 3A). The duration of the study has no impact on the permeability of each treatment under the RSNO form while the permeability under the nitrite ions and nitrate ions (the oxidation product of nitrite ions) forms depended on time (Fig. 3B and 3C, $p_{time} < 0.05$) and on the treatment. Indeed, the NACNO treatment induced a higher absorption of NO_2^- (and NO_3^-) ionic forms than the GSNO and the SNAP treatments ($p_{treatment} = 0.0003$ and $p_{interaction}$ 0.0002), especially after 4 h ($p_{time} < 0.0001$) (Fig. 3B).

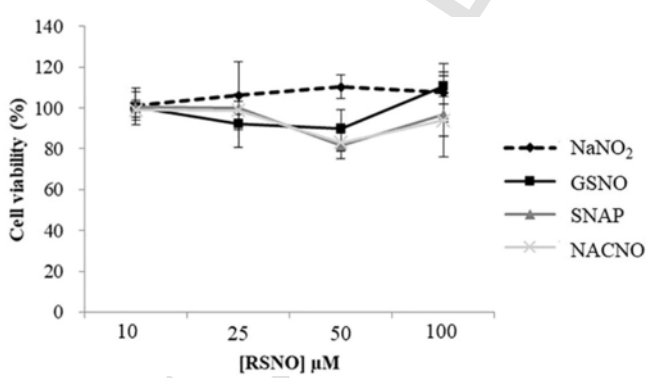

Fig. 2. Cytocompatibility of *S*-nitrosothiols with Caco-2 cells. Cell activity was assessed with the MTT test, 24 h after incubation with different *S*-nitrosothiols or $NaNO_2$. Values are expressed as mean ± SD of three independent experiments done in duplicate.

The $NaNO_2$ treatment led to the permeability of the two ionic species only (Fig. 3). The permeability under the NO_2^- form was time dependent and 30% higher than the permeability of each *S*-nitrosothiol treatment under NO_2^- form (Fig. 3B). The permeability under the nitrate ionic form (Fig. 3C), representing 5% of the initial amount, supposes a spontaneous oxidation of nitrite ions into nitrate ions within our experimental conditions (presence of dioxygen).

The Papp values for the NOx species (addition of RSNO, NO_2^- and NO_3^-) were situated within the medium class of permeability (BCS definition) for each *S*-nitrosothiol treatment and surrounded by the Papp values of the reference drugs, propranolol and furosemide (Table 2). The permeability of *S*-nitrosothiols under the RSNO form was 25–40 times lower (Papp ≈ 0.17×10^{-6} cm.s^{-1}) than that of NOx species, confirming the higher absorption of *S*-nitrosothiols under the NO_2^- and NO_3^- ionic forms. The $NaNO_2$ treatment allowed to define a high permeability under the NO_2^- ionic form.

After 4 h of permeability, 60% of the initial amount (50 nmol) of *S*-nitrosothiols remained in the apical compartment for the GSNO and SNAP treatments, and only 10% for the NACNO treatment (Fig. 4A). Furthermore, the NACNO treatment led to a higher amount of nitrite ions remaining in the apical compartment compared to the GSNO and SNAP treatments (Fig. 4B), suggesting a higher degradation of NACNO into NO_2^-. Non-permeated nitrate ions amounts were around 23% for each treatment (Fig. 4C). The $NaNO_2$ treatment was still presenting 41% of non-permeated nitrite ions after 4 h (Fig. 4B) and lower spontaneous oxidation into nitrate ions (4%) within the apical compartment compared to *S*-nitrosothiol treatments (Fig. 4C).

Finally, the calculation of the mass balance (addition of all species quantified in the two compartments) after 4 h of permeability study, showed 83 ± 16% to 106 ± 13% of recovery for GSNO, SNAP and $NaNO_2$ (Table 3). Nevertheless, the NACNO treatment showed a loss of 23% of the initial amount deposited in the apical compartment. This missing can be trapped inside the cell monolayer, so cells were lysed and only RSNO and nitrite ions were quantified. Indeed, due to intracellular reducing power [35], the nitrate ions cannot exist inside cells. Quantities of RSNO found inside the cells were higher for *S*-nitrosothiol treatments than for the $NaNO_2$ treatment (Fig. 5A). This was the opposite for the NO_2^- intake (Fig. 5B). For each *S*-nitrosothiol treatment, the intracellular incorporation of the RSNO form was higher than the nitrite ions form. Intracellular quantity of the RSNO form depended on the *S*-nitrosothiol chemical structure ($p_{treatment} < 0.05$) with the lowest incorporation obtained for the SNAP treatment (< 2% of the initial amount) (Fig. 5A). Intracellular incorporation of nitrite ions was independent on time and treatments (Fig. 5B).

For intracellular quantification, the surface area of cells was increased 4.17 times (from 1.12 to 4.67 cm^2) in order to be able to quantify NOx species inside the cells. So, the intracellular amounts of RSNO and NO_2^- form were divided by 4.17 to calculate the mass balance (Table 2). The intracellular incorporation of RSNO and NO_2^- represented only 1.1%, 1.0% and 0.4% of the initial amount, for the GSNO, NACNO and SNAP treatments, respectively. Therefore, 22% of the initial amount are still missing for the NACNO treatment.

UNCORRECTED PROOF

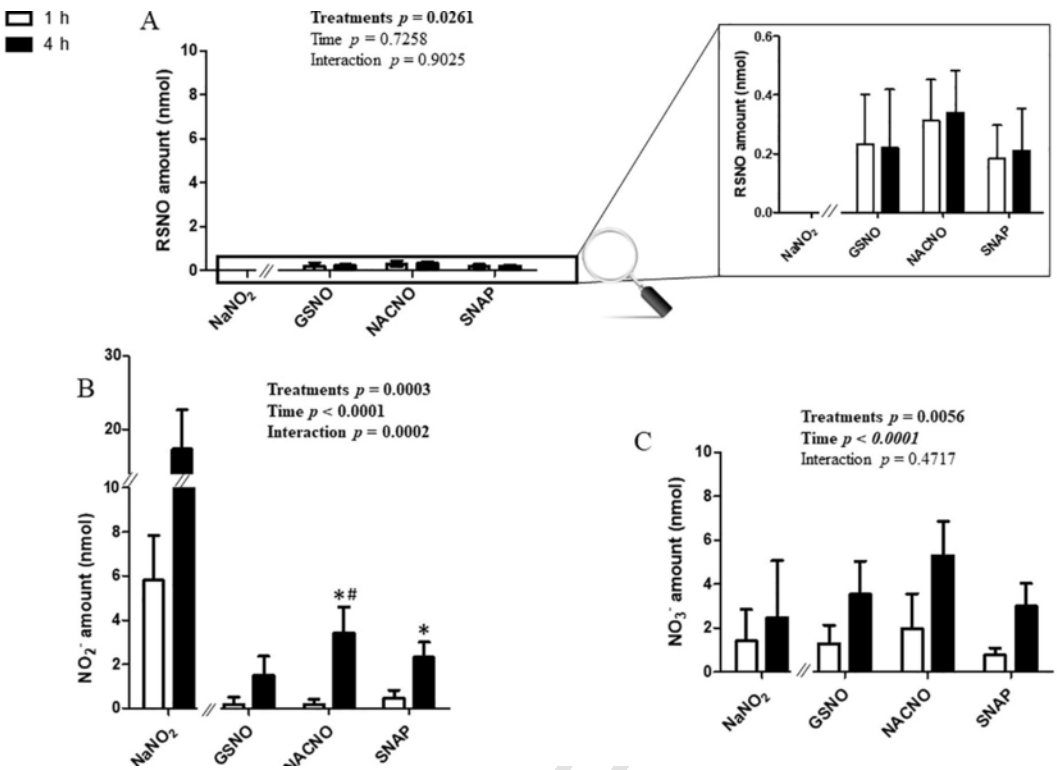

Fig. 3. Apical (pH 7.4) to basolateral compartment – Quantification in the basolateral compartment of permeated (A) RSNO, (B) NO_2^- and (C) NO_3^- after 1 h and 4 h of exposure to 50 nmol of each treatment. Results are shown as mean ± SD of four independent experiments done in duplicate and are compared using two-way ANOVA ($p_{treatment}$ (GSNO, NACNO, SNAP; excluding $NaNO_2$), p_{time} (1h, 4h) and $p_{interaction}$). * *vs.* GSNO; # *vs.* SNAP at the same time; $p < 0.05$ (Bonferroni's multiple comparisons test).

Table 2
Values of apparent permeability coefficient (Papp) for NOx species (RSNO + NO_2^- + NO_3^-) and the RSNO molecular form after 4 h of permeation from the apical to the basolateral compartment. nd: not determined, LOQ: Limit of quantification. Mean ± SD of four independent experiments done in duplicate.

Treatments	NOx Papp ($\times 10^{-6}$ cm.s^{-1})	RSNO Papp ($\times 10^{-6}$ cm.s^{-1})
GSNO	2.6 ± 0.9	0.2 ± 0.1
NACNO	5.0 ± 2.1	0.21 ± 0.08
SNAP	3.3 ± 1.6	0.13 ± 0.09
$NaNO_2$	12.3 ± 3.2	Under LOQ
Propranolol	24.4 ± 1	nd
Furosemide	0.3 ± 0.1	nd

3.3. *S-Nitrosothiols permeability from the basolateral to apical compartment*

In order to determine the permeability modality (passive *vs.* active) for each *S*-nitrosothiol, the study was carried out in the opposite direction, from the basolateral to the apical compartment.

In this condition, the permeability of the RSNO form (Fig. 6A) was only dependent on time for each *S*-nitrosothiol treatment. The permeability of the NO_2^- and NO_3^- ionic forms was dependent on time and treatment (Fig. 6B and 6C). Higher amounts were permeated under the NO_2^- ionic form for the NACNO and SNAP treatments (≈ 3% of initial amounts) compared to the GSNO treatment (1.2% of initial amount, Fig. 6B). As in the experiments performed from the apical to the basolateral compartment (Section 3.2), NO_2^- and NO_3^- were the major permeated species.

For each *S*-nitrosothiol treatment, the Papp values in both directions (apical to basolateral versus basolateral to apical) were equivalent (Tables 2 and 4), the *S*-nitrosothiols intestinal permeability can be postulated as a passive diffusion [36]. This postulate is also based on the validation of our intestinal barrier model comparing the Papp values of reference molecules with the literature [19]. Propranolol with equivalent bidirectional Papp values follows a passive diffusion whereas furosemide with a higher Papp value from basolateral to apical than from apical to basolateral, follows an active efflux transport.

After 4 h of permeability study, 95% of the initial amount (150 nmol) of each *S*-nitrosothiol treatment remained unpermeated (Fig. 7). The amounts of unpermeated NO_2^- ions (Fig. 7B) were the only form that depended on *S*-nitrosothiol chemical structure ($p_{treatment} = 0.0344$). As *S*-nitrosothiols are separated from cells by the porous membrane of the device, they cannot be metabolised by cell membrane enzymes showing the great importance of *S*-nitrosothiol metabolism in their permeability. Furthermore, the high amount of remaining RSNO form (Fig. 7A) attested from the stability of each *S*-nitrosothiol in our operating conditions.

This also showed that the degradation of *S*-nitrosothiols into ionic forms observed in the apical to basolateral permeability study (Fig. 4) was due to cell membrane enzymes activity. Finally, the study of *S*-nitrosothiols permeability from the basolateral to the apical compartment showed a mass balance of 100% for each *S*-nitrosothiol treatment (Table 5).

3.4. *Influence of the apical pH on S-nitrosothiols permeability*

The principal site of absorption of small molecules including peptides and amino acids is the jejunum part of the intestine, which physiological pH ranges from 6 to 7. In order to study the permeability of *S*-nitrosothiols close to physiological conditions, the pH of the apical compartment mimicking the intestinal lumen was shifted of one log from pH 7.4 to pH 6.4. pH acidification has no impact on propranolol

UNCORRECTED

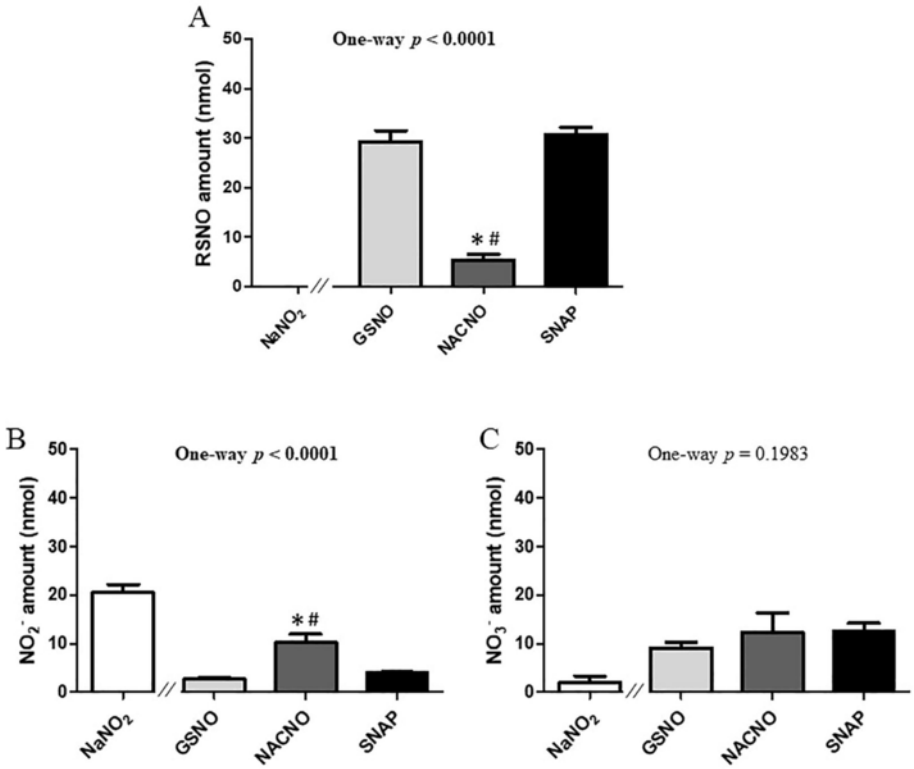

Fig. 4. Apical (pH 7.4) o basolateral compartment – Quantification in the apical compartment of remaining (A) RSNO, (B) NO_2^- and (C) NO_3^- and 4 h of exposure to 50 nmol of each treatment. Results are shown as mean ± SD of four independent experiments done in duplicate and are compared using one-way ANOVA (excluding $NaNO_2$) Bonferroni post-test. * *vs.* GSNO; # *vs.* SNAP at the same time; $p < 0.05$.

Table 3
Mass balance for each treatment (initial amount: 50 nmol) after 4 h of permeation from the apical to the basolateral compartment. Mean ± SD of four independent experiments done in duplicate.

Treatments	Amount (nmol)	Percentage of initial amount
GSNO	46 ± 4	92 ± 8
NACNO	38 ± 6	77 ± 12
SNAP	53 ± 7	106 ± 13
$NaNO_2$	41 ± 8	83 ± 16

and furosemide permeability [27], so the experiment was not performed.

At pH 6.4, the permeability of each *S*-nitrosothiol under the RSNO and the ionic forms (Fig. 8) followed the same profile than at pH 7.4 (Fig. 3). However, the NACNO treatment showed a 7 times increase of permeability under the RSNO form (Fig. 8A) compared to pH 7.4. The $NaNO_2$ treatment showed a permeability under the RSNO form (Fig. 8A) and a large (10 times at 1 h and 20 times at 4 h) increase of the permeability under the NO_3^- form (Fig. 8C). So, at pH 6.4, the Papp values of NOx species and RSNO form rose for the $NaNO_2$ treatment (Table 6) compared to pH 7.4 (Table 2).

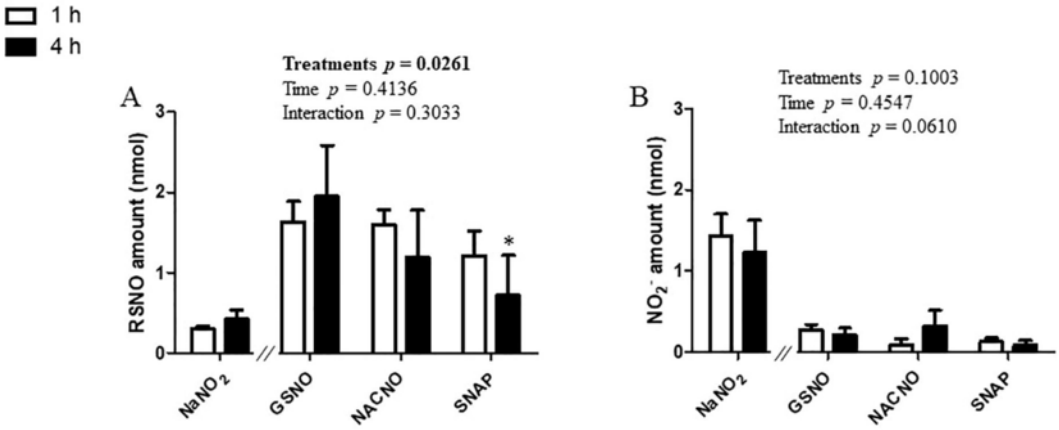

Fig. 5. Apical (pH 7.4) to basolateral permeability – Intracellular quantifications of (A) RSNO, (B) NO_2^-, (subtracted from the control cells) after 1 h and 4 h of exposure to 50 nmol of each treatment. Results are shown as mean ± SD of four independent experiments done in duplicate and are compared using two-way ANOVA ($p_{treatment}$ (GSNO, NACNO, SNAP; excluding $NaNO_2$), p_{time} (1h, 4h) and $p_{interaction}$). * *vs.* GSNO at the same time; $p < 0.05$ (Bonferroni's multiple comparisons test).

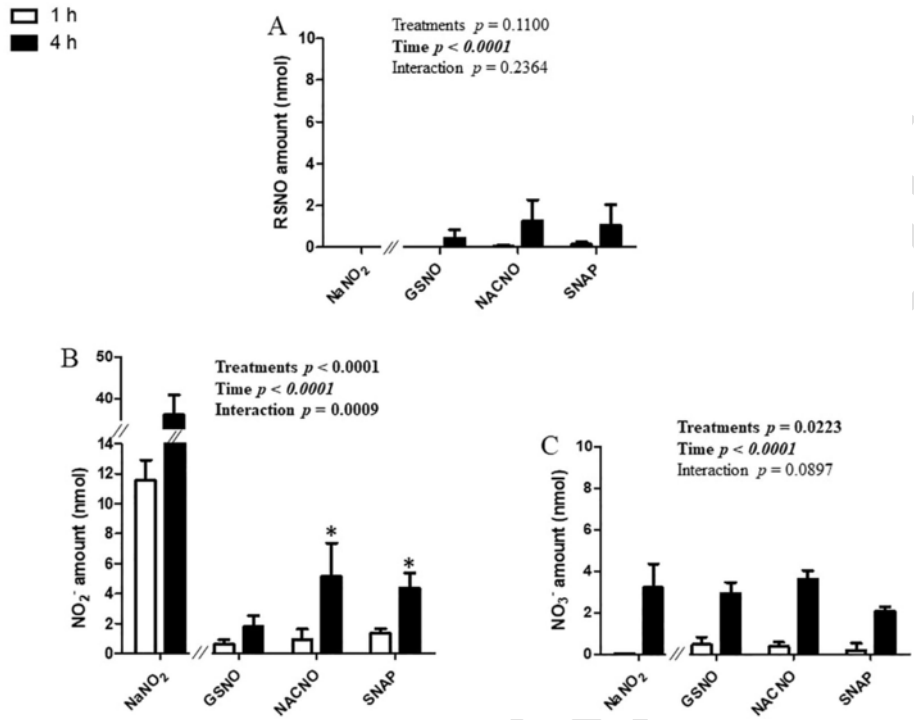

Fig. 6. Basolateral to Apical permeability – Quantification in the apical compartment of permeated (A) RSNO, (B) NO_2^- and (C) NO_3^- after 1 h and 4 h from 150 nmol of each treatment. Results are shown as mean ± SD of four independent experiments done in duplicate and are compared using two-way ANOVA ($p_{treatment}$ (GSNO, NACNO, SNAP; excluding $NaNO_2$), p_{time} (1h, 4 h) and $p_{interaction}$). * *vs.* GSNO at the same time; $p < 0.05$ (Bonferroni's multiple comparisons test).

Table 4
Values of apparent permeability coefficient (Papp) for NOx species (RSNO + NO_2^- + NO_3^-) and the RSNO form after 4 h of permeation from basolateral to apical compartment. nd: not determined, LOQ: Limit of quantification. Mean ± SD of four independent experiments done in duplicate.

Treatments	NOx Papp ($\times 10^{-6}$ cm.s^{-1})	RSNO Papp ($\times 10^{-6}$ cm.s^{-1})
GSNO	2.8 ± 1.2	0.3 ± 0.2
NACNO	4.5 ± 1.5	0.6 ± 0.6
SNAP	4.1 ± 0.7	0.5 ± 0.5
$NaNO_2$	97.5 ± 16.4	Under LOQ
Propranolol	33.1 ± 0.8	nd
Furosemide	15.2 ± 0.8	nd

The Papp values at pH 6.4 (Table 6) maintained each *S*-nitrosothiol in the medium class of permeability for NOx species and in the low permeability class for the RSNO form. However, the Papp value of the NACNO treatment under the RSNO form increased from $0.21 \pm 0.08 \times 10^{-6}$ cm.s^{-1} (Table 2) at pH 7.4 to $0.9 \pm 0.7 \times 10^{-6}$ cm.s^{-1} at pH 6.4, bringing NACNO close to the medium permeability class (from 1 to 10×10^{-6} cm.s^{-1}, [19]).

The distribution of non-permeated species remaining in the apical compartment after 4 h of permeability at pH 6.4 (Fig. 9) was similar to that at pH 7.4 (Fig. 4).

The absorption of *S*-nitrosothiols from the apical compartment at pH 6.4 to the basolateral compartment at pH 7.4 presented a mass balance from 58% to 78% of the initial amount (Table 7).

4. Discussion

The human intestinal barrier model based on Caco-2 cells is widely used in the pharmaceutical industry to determine the parameters of intestinal permeability of new drugs. The results obtained depend mainly on cell culture parameters (time, medium and age [29]). In the present study, we validated our conditions using two reference molecules, *i.e.* propranolol and furosemide, in comparison with already published Papp values. These Papp values, as well as TEER values (> 500 Ω.cm^2), are quality guaranties of our model and results. From the literature, propranolol, with a Papp value between 3.30×10^{-6} and 41.90×10^{-6} cm.s^{-1} [26,27] belongs to the high permeability class, and furosemide, with a Papp value varying from 0.04×10^{-6} to 0.11×10^{-6} cm.s^{-1} [26,37] belongs to the low permeability class. Such a low permeability for furosemide was attributed to an efflux driven by the intestinal P-glycoprotein to the luminal direction [38]. The Papp values for propranolol (24.4×10^{-6} cm.s^{-1}) and furosemide (0.3×10^{-6} cm.s^{-1}) obtained using our intestinal barrier model confirm the already published values and probably attest for the presence and activity of the P-glycoprotein in this model.

S-Nitrosothiols are NO donors allowing the release of NO with a relative short half-life (within a few hours) [2]. Thereby, in aqueous medium, NO is spontaneously and quickly oxidized into nitrite and nitrate ions. So, it is mandatory to study the intestinal permeability of these ionic species as well as the permeability of the RSNO form to evaluate the bioavailability of NO in the blood stream after oral administration. In the present study, each *S*-nitrosothiol increased their permeability following time, in each of the three proposed conditions (apical to basolateral compartments at pH 7.4 direction, opposite direction, apical compartment at pH 6.4 to basolateral compartment at pH 7.4).

The study of *S*-nitrosothiols permeability from the compartment mimicking the intestinal lumen (apical compartment) to the compartment mimicking the lumen of blood vessels (basolateral compartment) revealed a weak absorption of each *S*-nitrosothiol treatment under the RSNO form compared to the ionic species, which are the major absorbed species (Fig. 10A). In a general point of view, the ionic species are more absorbed by the intestine than the neutral molecules. Indeed, specific ionic transporters such as the Organic Cation

UNCORRECTED PROOF

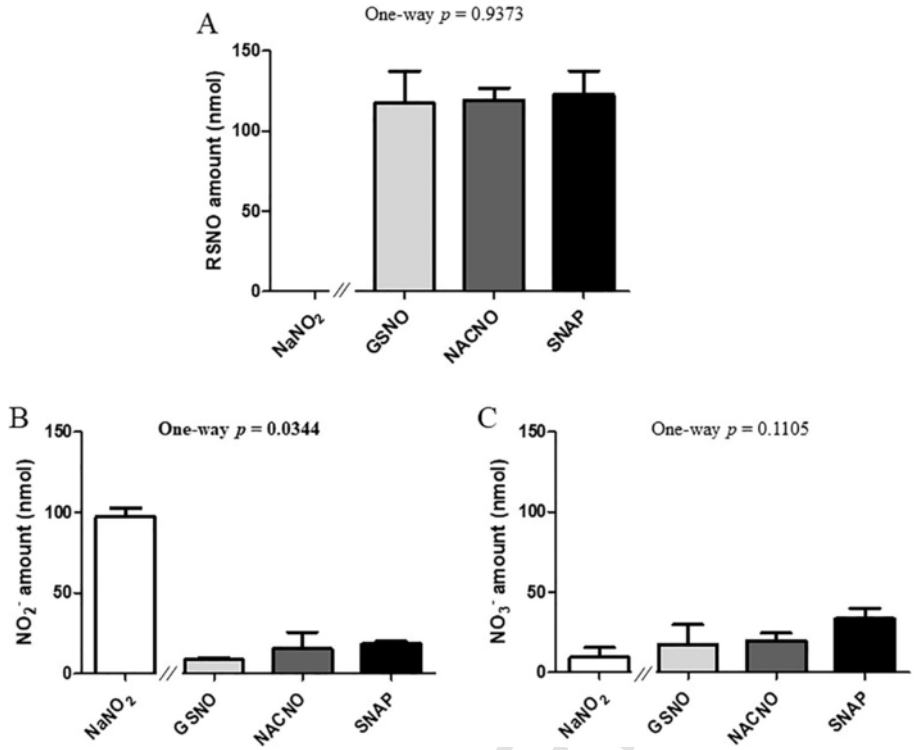

Fig. 7. Basolateral to apical permeability – Quantification in the basolateral compartment of remaining (A) RSNO, (B) NO_2^- and (C) NO_3^- after 4 h of exposure to 150 nmol of each treatment. Results are shown as mean ± SD of four independent experiments done in duplicate and are compared using one-way ANOVA (excluding $NaNO_2$).

Table 5
Mass balance for each tested treatment (initial amount 150 nmol) after 4 h of permeability from the basolateral to the apical compartment. Mean ± SD of four independent experiments done in duplicate.

Treatments	Amount (nmol)	Percentage of the initial amount
GSNO	169 ± 40	113 ± 36
NACNO	159 ± 24	106 ± 21
SNAP	162 ± 49	108 ± 44
$NaNO_2$	155 ± 18	103 ± 17

Transporters (OCT) and the Zwitterion Transporters (OCTN), implied in the absorption of Na^+ and Ca^{2+}, are expressed within the intestinal tissue and Caco-2 cells [39,40].

The Papp values of all permeated species placed each *S*-nitrosothiol studied within the medium permeability class for NOx species, class that was surrounded by our two reference molecules (propranolol and furosemide). The Papp value was the same for each *S*-nitrosothiol even if they presented different physico-chemical properties with a higher hydrophilicity for GSNO than SNAP [2]. In this way, the physico-chemical properties of the skeleton (R) carrying the nitroso group are not prevalent for the intestinal permeability of the *S*-nitrosothiols. The mass balance within both compartments allowed a recovery of 100% of the initial amount deposited for the SNAP treatment. The small missing amount for the GSNO treatment was recovered by the intracellular quantification, rising the mass balance to almost 100%. However, the NACNO treatment showed a mass balance of 75%, which was not completed to 100% after intracellular quantification.

The amount of NOx species found inside the cells was higher for the GSNO treatment than for the SNAP treatment, with the NACNO treatment situated between each other. SNAP promotes drug intestinal absorption [41] by opening tight junctions without affecting barrier integrity. Indeed, SNAP increases insulin rectal absorption, transepithelial transport of fluorescein sulfonic acid (low absorbable molecule) [41,42] and macromolecules absorption through the intestine by the reversible opening of tight junctions [41,43,44] and a thickening of ileal mucosal membrane [45]. So, in our study, paracellular absorption of SNAP can be speculated. GSNO and NACNO were partially absorbed *via* a transcellular pathway. The mass imbalance observed for the NACNO treatment can be attributed to its higher metabolism within the apical compartment. Moreover, the metabolism of each *S*-nitrosothiol was abolished in the donor compartment when studying the permeability from the basolateral to the apical compartments. This phenomenon is a proof of the intestinal barrier orientation with a brush border including metabolic enzymes like redoxins and gamma-glutamyl transferase [46], faced to the apical compartment, and a basal lamina without any metabolic activity faced to the basolateral compartment.

The equal Papp values obtained permeability studies from the apical to the basolateral compartments and permeability studies from the basolateral to the apical compartments revealed that the absorption of *S*-nitrosothiols is driven by a passive diffusion through the intestinal barrier (Fig. 10B). This transport modality excluded the participation of all transport systems and energy consumption in the permeability of *S*-nitrosothiols [47]. In that way, *S*-nitrosothiols permeability may be improved using pharmaceutical formulations, which are aimed at opening tight junctions and increasing the local concentration and the residence time of the molecule.

Finally, the acidification (pH 6.4) of the apical compartment to mimic the physiological condition of the jejunum part of the intestine (Fig. 10C) showed a permeability dependent on the *S*-nitrosothiol treatment. The very low permeability of the RSNO form for the NACNO treatment at pH 7.4 was multiplied by ten at pH 6.4. However, this favoured permeability of NACNO seemed to be related neither to the lipophilic balance – as NACNO showed a log P intermediate between GSNO and SNAP – nor to the ionization state – as the isoelectric point (pI) of NACNO is intermediate (3.24) between

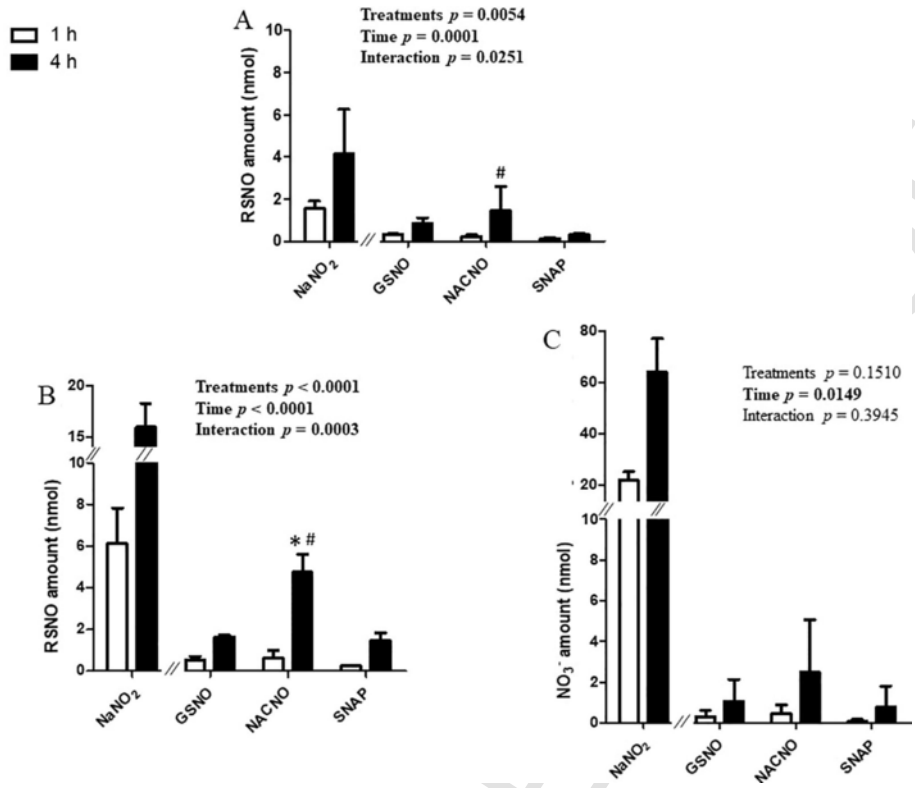

Fig. 8. Apical pH 6.4 to Basolateral permeability – Quantification in the basolateral compartment of remaining (A) RSNO, (B) NO_2^- and (C) NO_3^- after 1 h and 4 h of exposure to 50 nmol of each treatment. Results are shown as mean ± SD of three independent experiments done in duplicate and are compared using two-way ANOVA ($p_{treatment}$ (GSNO, NACNO, SNAP; excluding $NaNO_2$), p_{time} (1h, 4h) and $p_{interaction}$). * *vs.* GSNO; # *vs.* SNAP at the same time; $p < 0.05$ (Bonferroni's multiple comparisons test).

Table 6
Values of apparent permeability coefficient (Papp) for NOx species (RSNO + NO_2^- + NO_3^-) and the RSNO form after 4 h of permeability study from the apical compartment (pH 6.4) to the basolateral compartment (pH 7.4). Mean ± SD of three independent experiments done in duplicate.

Treatments	NOx Papp ($\times 10^{-6}$ cm.s^{-1})	RSNO Papp ($\times 10^{-6}$ cm.s^{-1})
GSNO	1.9 ± 0.6	0.5 ± 0.2
NACNO	4.8 ± 2.4	0.9 ± 0.7
SNAP	1.4 ± 0.8	0.20 ± 0.05
$NaNO_2$	207.0 ± 37.9	7.7 ± 6.5

GSNO and SNAP (4.8 and 4.85, respectively) and far away from the studied pHs. As the thiol functions are blocked by NO, their pKa values are not involved in the pI of the *S*-nitrosothiols. However, it may be involved in the stability of the S-NO bound, *e.g* the *S*-nitrosocysteine (cysNO) is less stable than GSNO due to a lower pKa of the thiol function of the cysteine residue. The permeability of the RSNO form for the $NaNO_2$ treatment suggested that pH 6.4 favoured the formation of RSNO starting from NO_2^-. This can also be postulated for all the experiments where permeability of the RSNO forms was observed. However, the formation of RSNO following the $NaNO_2$ treatment should certainly occur thanks to intracellular thiols, which are the only available source of thiol in the experimental system. This phenomenon will lead to cell thiol depletion, which will induce tolerance at it was already seen in clinics for organic nitrate treatments [48]. However, our experiments showed that *S*-nitrosothiol treatments bringing the thiol function itself, won't induce thiol depletion neither tolerance phenomenon. Furthermore, Pinheiro and coworkers demonstrated that oral administration of nitrite ions allowed the formation of RSNO in the stomach leading to an increased plasma RSNO concentration [17]. Our work precises that the formation of RSNO may also occur in the jejunum part of the intestine at acidic pH.

Finally, according to the BCS, *S*-nitrosothiols can be classified between class I and class III, regarding their high solubility and medium permeability. From Le Ferrec et al. [49], the result obtained *in vitro* with high permeability molecules (class I and class II) can be easily transposed to *in vivo* intestinal absorption unlike results obtained for low permeability molecules (class III and class IV). So, the *S*-nitrosothiols included in the medium class of permeability can be considered as drugs suitable for oral administration. Thereafter, it would be interesting to study the permeability of *S*-nitrosothiols in the presence of albumin in the basolateral compartment to mimic the blood stream compartment [50]. Furthermore, albumin including a free reduced cysteine residue in position 34 will increase the amount of RSNO found in the basolateral compartment through *S*-nitrosation process.

In conclusion, our study suggested that *S*-nitrosothiols can be administrated by the oral route to be absorbed at the intestinal level, mainly in the jejunum part. The passive diffusion of *S*-nitrosothiols under three different kinds of species such as nitrite and nitrate ions and the RSNO form was demonstrated using a model of human intestinal barrier. The permeation of the RSNO species will improve the interest for *S*-nitrosothiols oral administration compared to nitrite ions. Indeed, *S*-nitrosothiols would not deplete the intracellular stock of reduced thiols. Even if *S*-nitrosothiols are good candidates for NO oral supplementation, they will need appropriate protection from enzymatic degradation using nanotechnologies [20,51–53].

Acknowledgments

The authors acknowledge Dr Wen WU for her help in preliminary experiment settings. The CITHEFOR EA3452 lab was supported by the

UNCORRECTED PROOF

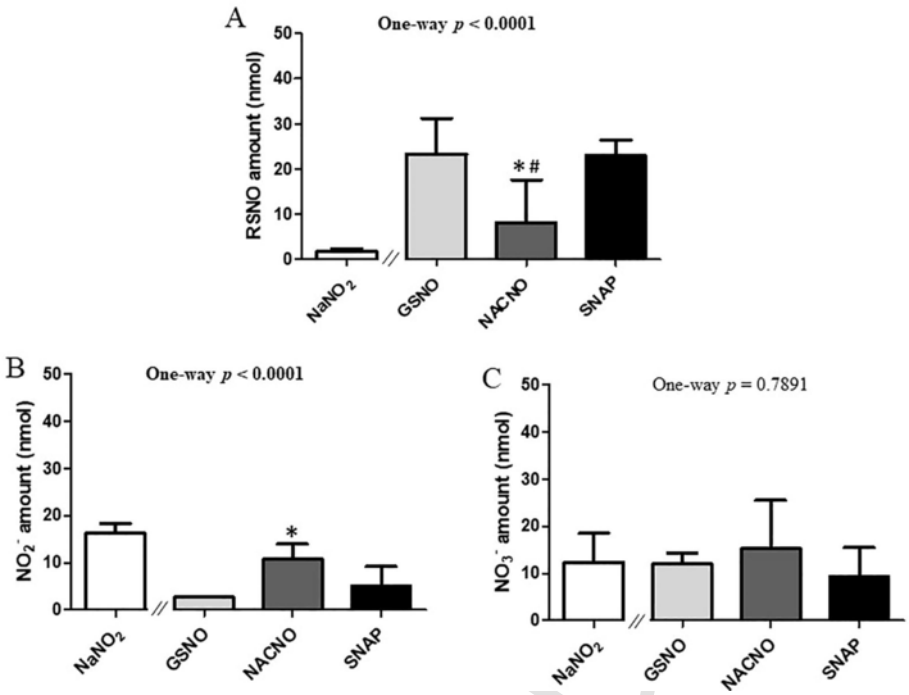

Fig. 9. Apical (pH 6.4) to basolateral compartment – Quantification in the apical compartment of remaining (A) RSNO, (B) NO_2^- and (C) NO_3^- after 1 h and 4 h of exposure to 50 nmol of each treatment. Results are shown as mean ± SD of three independent experiments done in duplicate and are compared using one-way ANOVA (excluding $NaNO_2$). * *vs.* GSNO; # *vs.* SNAP at the same time; $p < 0.05$ (Bonferroni post-test).

Table 7
Mass balance for all tested treatments (initial amount 50 nmol) after 4 h of permeability from the apical compartment at pH 6.4 to the basolateral compartment at pH 7.4. Mean ± SD of three independent experiments done in duplicate.

Treatments	Amount (nmol)	Percentage of the initial amount
GSNO	34 ± 10	68 ± 20
NACNO	37 ± 10	78 ± 20
SNAP	31 ± 5	58 ± 8
$NaNO_2$	114 ± 18	227 ± 35

"Impact Biomolecules" project of the "*Lorraine Université d'Excellence*" (*Investissements d'avenir – ANR*).

UNCORRECTED PROOF

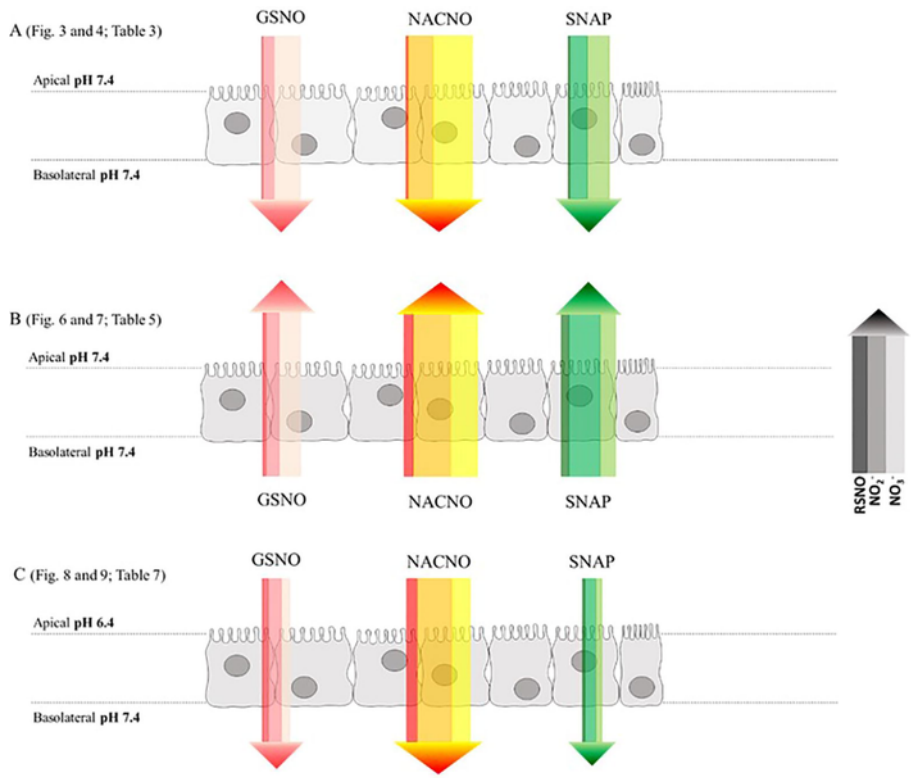

Fig. 10. Summary of NOx species permeability for each *S*-nitrosothiol treatment. The colour code of each arrow from the left to the right is the amount (width) of RSNO, NO_2^- and NO_3^-. The 4 h-permeability for each treatment is represented from (A) apical to basolateral compartment, (B) basolateral to apical compartment and (C) apical (pH 6.4) to basolateral compartment (pH 7.4).

References

[1] T.S. Hakim, K. Sugimori, E.M. Camporesi, G. Anderson, Half-life of nitric oxide in aqueous solutions with and without haemoglobin, Physiol. Meas. 17 (1996) 267–277.

[2] C. Gaucher, A. Boudier, F. Dahboul, M. Parent, P. Leroy, S-nitrosation/denitrosation in cardiovascular pathologies: facts and concepts for the rational design of S-nitrosothiols, Curr. Pharm. Des. 19 (2013) 458–472.

[3] Z. Kaposzta, P.A. Baskerville, D. Madge, S. Fraser, J.F. Martin, H.S. Markus, L-Arginine and S-nitrosoglutathione reduce embolization in humans, Circulation 103 (2001) 2371–2375.

[4] Z. Kaposzta, A. Clifton, J. Molloy, J.F. Martin, H.S. Markus, S-nitrosoglutathione reduces asymptomatic embolization after carotid angioplasty, Circulation 106 (2002) 3057–3062.

[5] Z. Kaposzta, J.F. Martin, H.S. Markus, Switching off embolization from symptomatic carotid plaque using S-nitrosoglutathione, Circulation 105 (2002) 1480–1484.

[6] T. Rassaf, P. Kleinbongard, M. Preik, A. Dejam, P. Gharini, T. Lauer, J. Erckenbrecht, A. Duschin, R. Schulz, G. Heusch, M. Feelisch, M. Kelm, Plasma nitrosothiols contribute to the systemic vasodilator effects of intravenously applied NO: experimental and clinical Study on the fate of NO in human blood, Circ. Res. 91 (2002) 470–477.

[7] T. Rassaf, L.W. Poll, P. Brouzos, T. Lauer, M. Totzeck, P. Kleinbongard, P. Gharini, K. Andersen, R. Schulz, G. Heusch, U. Mödder, M. Kelm, Positive effects of nitric oxide on left ventricular function in humans, Eur. Heart J. 27 (2006) 1699–1705, https://doi.org/10.1093/eurheartj/ehl096.

[8] S. Moncada, A. Higgs, The L-arginine-nitric oxide pathway, N. Engl. J. Med. 329 (1993) 2002–2012, https://doi.org/10.1056/NEJM199312303292706.

[9] B. Meyer, A. Genoni, A. Boudier, P. Leroy, M.F. Ruiz-Lopez, Structure and stability studies of pharmacologically relevant S-nitrosothiols: a theoretical approach, J. Phys. Chem. A 120 (2016) 4191–4200, https://doi.org/10.1021/acs.jpca.6b02230.

[10] B.A. Maron, S.-S. Tang, J. Loscalzo, S-nitrosothiols and the S-nitrosoproteome of the cardiovascular system, Antioxid. Redox Signal. 18 (2013) 270–287, https://doi.org/10.1089/ars.2012.4744.

[11] E. Belcastro, W. Wu, I. Fries-Raeth, A. Corti, A. Pompella, P. Leroy, I. Lartaud, C. Gaucher, Oxidative stress enhances and modulates protein S-nitrosation in smooth muscle cells exposed to S-nitrosoglutathione, Nitric Oxide Biol. Chem. 69 (2017) 10–21, https://doi.org/10.1016/j.niox.2017.07.004.

[12] F. Dahboul, P. Leroy, K. Maguin Gate, A. Boudier, C. Gaucher, P. Liminana, I. Lartaud, A. Pompella, C. Perrin-Sarrado, Endothelial γ-glutamyltransferase contributes to the vasorelaxant effect of S-nitrosoglutathione in rat aorta, PloS One 7 (2012)e43190https://doi.org/10.1371/journal.pone.0043190.

[13] M.H. Krieger, K.F.R. Santos, S.M. Shishido, A.C.B.A. Wanschel, H.F.G. Estrela, L. Santos, M.G. De Oliveira, K.G. Franchini, R.C. Spadari-Bratfisch, F.R.M. Laurindo, Antiatherogenic effects of S-nitroso-N-acetylcysteine in hypercholesterolemic LDL receptor knockout mice, Nitric Oxide Biol. Chem. 14 (2006) 12–20, https://doi.org/10.1016/j.niox.2005.07.011.

[14] M. Khan, B. Sekhon, S. Giri, M. Jatana, A.G. Gilg, K. Ayasolla, C. Elango, A.K. Singh, I. Singh, S-Nitrosoglutathione reduces inflammation and protects brain against focal cerebral ischemia in a rat model of experimental stroke, J. Cereb. Blood Flow Metab. Off. J. Int. Soc. Cereb. Blood Flow Metab. 25 (2005) 177–192, https://doi.org/10.1038/sj.jcbfm.9600012.

[15] M. Khan, M. Jatana, C. Elango, A.S. Paintlia, A.K. Singh, I. Singh, Cerebrovascular protection by various nitric oxide donors in rats after experimental stroke, Nitric Oxide Biol. Chem. 15 (2006) 114–124, https://doi.org/10.1016/j.niox.2006.01.008.

[16] M. Khan, T.S. Dhammu, M. Baarine, J. Kim, M.K. Paintlia, I. Singh, A.K. Singh, GSNO promotes functional recovery in experimental TBI by stabilizing HIF-1α, Behav. Brain Res. 340 (2018) 63–70, https://doi.org/10.1016/j.bbr.2016.10.037.

[17] L.C. Pinheiro, J.H. Amaral, G.C. Ferreira, R.L. Portella, C.S. Ceron, M.F. Montenegro, J.C. Toledo, J.E. Tanus-Santos, Gastric S-nitrosothiol formation drives the antihypertensive effects of oral sodium nitrite and nitrate in a rat model of renovascular hypertension, Free Radic. Biol. Med. 87 (2015) 252–262, https://doi.org/10.1016/j.freeradbiomed.2015.06.038.

[18] M. Levin (Ed.), Pharm. Process Scale-Up, Informa Healthcare, 2001https://doi.org/10.1201/9780824741969.axh.

[19] Y. Peng, P. Yadava, A.T. Heikkinen, N. Parrott, A. Railkar, Applications of a 7-day Caco-2 cell model in drug discovery and development, Eur. J. Pharm. Sci. Off. J. Eur. Fed. Pharm. Sci. 56 (2014) 120–130, https://doi.org/10.1016/j.ejps.2014.02.008.

[20] W. Wu, C. Perrin-Sarrado, H. Ming, I. Lartaud, P. Maincent, X.-M. Hu, A. Sapin-Minet, C. Gaucher, Polymer nanocomposites enhance S-nitrosoglutathione intestinal absorption and promote the formation of releasable nitric oxide stores in rat aorta, Nanomed. Nanotechnol. Biol. Med. 12 (2016) 1795–1803, https://doi.org/10.1016/j.nano.2016.05.006.

[21] K.A. Broniowska, A.R. Diers, N. Hogg, S-nitrosoglutathione, Biochim. Biophys. Acta. 2013 (1830) 3173–3181, https://doi.org/10.1016/j.bbagen.2013.02.004.

[22] P. Teixeira, P. Napoleão, C. Saldanha, S-nitrosoglutathione efflux in the erythrocyte, Clin. Hemorheol. Microcirc. 60 (2015) 397–404, https://doi.org/10.3233/CH-141855.
[23] L.F. Prescott, R.N. Illingworth, J.A. Critchley, M.J. Stewart, R.D. Adam, A.T. Proudfoot, Intravenous N-acetylcystine: the treatment of choice for paracetamol poisoning, Br. Med. J. 2 (1979) 1097–1100.
[24] Y. Wang, J. Cao, X. Wang, S. Zeng, Stereoselective transport and uptake of propranolol across human intestinal Caco-2 cell monolayers, Chirality 22 (2010) 361–368, https://doi.org/10.1002/chir.20753.
[25] M. Parent, A. Boudier, F. Dupuis, C. Nouvel, A. Sapin, I. Lartaud, J.-L. Six, P. Leroy, P. Maincent, Are in situ formulations the keys for the therapeutic future of S-nitrosothiols?, Eur. J. Pharm. Biopharm. Off. J. Arbeitsgemeinschaft Pharm. Verfahrenstechnik EV 85 (2013) 640–649, https://doi.org/10.1016/j.ejpb.2013.08.005.
[26] E.H. Kerns, L. Di, S. Petusky, M. Farris, R. Ley, P. Jupp, Combined application of parallel artificial membrane permeability assay and Caco-2 permeability assays in drug discovery, J. Pharm. Sci. 93 (2004) 1440–1453, https://doi.org/10.1002/jps.20075.
[27] C. Zhu, L. Jiang, T.-M. Chen, K.-K. Hwang, A comparative study of artificial membrane permeability assay for high throughput profiling of drug absorption potential, Eur. J. Med. Chem. 37 (2002) 399–407.
[28] S.I. Khan, E.A. Abourashed, I.A. Khan, L.A. Walker, Transport of harman alkaloids across Caco-2 cell monolayers, Chem. Pharm. Bull. (Tokyo) 52 (2004) 394–397.
[29] B. Srinivasan, A.R. Kolli, M.B. Esch, H.E. Abaci, M.L. Shuler, J.J. Hickman, TEER measurement techniques for in vitro barrier model systems, J. Lab. Autom. 20 (2015) 107–126, https://doi.org/10.1177/2211068214561025.
[30] W.S. Jobgen, S.C. Jobgen, H. Li, C.J. Meininger, G. Wu, Analysis of nitrite and nitrate in biological samples using high-performance liquid chromatography, J. Chromatogr. B Analyt. Technol. Biomed. Life. Sci. 851 (2007) 71–82, https://doi.org/10.1016/j.jchromb.2006.07.018.
[31] H.K. Kim, J.H. Hong, M.S. Park, J.S. Kang, M.H. Lee, Determination of propranolol concentration in small volume of rat plasma by HPLC with fluorometric detection, Biomed. Chromatogr. BMC 15 (2001) 539–545, https://doi.org/10.1002/bmc.110.
[32] G.S. Rekhi, S.S. Jambhekar, P.F. Souney, D.A. Williams, A fluorimetric liquid chromatographic method for the determination of propranolol in human serum/plasma, J. Pharm. Biomed. Anal. 13 (1995) 1499–1505.
[33] J.M. Ryu, S.J. Chung, M.H. Lee, C.K. Kim, C.K. Shim, Increased bioavailability of propranolol in rats by retaining thermally gelling liquid suppositories in the rectum, J. Control. Release Off. J. Control. Release Soc. 59 (1999) 163–172.
[34] T. Galaon, S. Udrescu, I. Sora, V. David, A. Medvedovici, High-throughput liquid-chromatography method with fluorescence detection for reciprocal determination of furosemide or norfloxacin in human plasma, Biomed. Chromatogr. 21 (2007) 40–47, https://doi.org/10.1002/bmc.715.
[35] O. Parodi, R. De Maria, E. Roubina, Redox state, oxidative stress and endothelial dysfunction in heart failure: the puzzle of nitrate-thiol interaction, J. Cardiovasc. Med. 8 (2007) 765–774, https://doi.org/10.2459/JCM.0b013e32801194d4.
[36] E.C. Sherer, A. Verras, M. Madeira, W.K. Hagmann, R.P. Sheridan, D. Roberts, K. Bleasby, W.D. Cornell, QSAR prediction of passive permeability in the LLC-PK1 cell line: trends in molecular properties and cross-prediction of Caco-2 permeabilities, Mol. Inform. 31 (2012) 231–245, https://doi.org/10.1002/minf.201100157.
[37] S. Yamashita, T. Furubayashi, M. Kataoka, T. Sakane, H. Sezaki, H. Tokuda, Optimized conditions for prediction of intestinal drug permeability using Caco-2 cells, Eur. J. Pharm. Sci. Off. J. Eur. Fed. Pharm. Sci. 10 (2000) 195–204.
[38] P.-A. Billat, E. Roger, S. Faure, F. Lagarce, Models for drug absorption from the small intestine: where are we and where are we going?, Drug Discov. Today. 22 (2017) 761–775, https://doi.org/10.1016/j.drudis.2017.01.007.
[39] T. Han, R.S. Everett, W.R. Proctor, C.M. Ng, C.L. Costales, K.L.R. Brouwer, D.R. Thakker, Organic cation transporter 1 (OCT1/mOct1) is localized in the apical membrane of caco-2 cell monolayers and enterocytes, Mol. Pharmacol. 84 (2013) 182–189, https://doi.org/10.1124/mol.112.084517.
[40] T. Hirano, S. Yasuda, Y. Osaka, M. Kobayashi, S. Itagaki, K. Iseki, Mechanism of the inhibitory effect of zwitterionic drugs (levofloxacin and grepafloxacin) on carnitine transporter (OCTN2) in Caco-2 cells, Biochim. Biophys. Acta BBA – Biomembr. 1758 (2006) 1743–1750, https://doi.org/10.1016/j.bbamem.2006.07.002.
[41] G. Fetih, F. Habib, H. Katsumi, N. Okada, T. Fujita, M. Attia, A. Yamamoto, Excellent absorption enhancing characteristics of NO donors for improving the intestinal absorption of poorly absorbable compound compared with conventional absorption enhancers, Drug Metab. Pharmacokinet. 21 (2006) 222–229.
[42] A. Yamamoto, H. Tatsumi, M. Maruyama, T. Uchiyama, N. Okada, T. Fujita, Modulation of intestinal permeability by nitric oxide donors: implications in intestinal delivery of poorly absorbable, Drugs 7 (2018).
[43] A.L. Salzman, M.J. Menconi, N. Unno, R.M. Ezzell, D.M. Casey, P.K. Gonzalez, M.P. Fink, Nitric oxide dilates tight junctions and depletes ATP in cultured Caco-2BBe intestinal epithelial monolayers, Am. J. Physiol. 268 (1995) G361–373, https://doi.org/10.1152/ajpgi.1995.268.2.G361.
[44] N. Numata, K. Takahashi, N. Mizuno, N. Utoguchi, Y. Watanabe, M. Matsumoto, T. Mayumi, Improvement of intestinal absorption of macromolecules by nitric oxide donor, J. Pharm. Sci. 89 (2000) 1296–1304.
[45] D.-Z. Xu, Q. Lu, E.A. Deitch, Nitric oxide directly impairs intestinal barrier function, Shock Augusta Ga 17 (2002) 139–145.
[46] N. Hogg, R.J. Singh, E. Konorev, J. Joseph, B. Kalyanaraman, S-Nitrosoglutathione as a substrate for gamma-glutamyl transpeptidase, Biochem. J. 323 (Pt 2) (1997) 477–481.
[47] B. Alberts, A. Johnson, J. Lewis, M. Raff, K. Roberts, P. Walter, Carrier Proteins and Active Membrane Transport, 2002. https://www.ncbi.nlm.nih.gov/books/NBK26896/ (accessed January 23, 2018).
[48] A. Daiber, T. Münzel, Organic nitrate therapy, nitrate tolerance, and nitrate-induced endothelial dysfunction: emphasis on redox biology and oxidative stress, Antioxid. Redox Signal. 23 (2015) 899–942, https://doi.org/10.1089/ars.2015.6376.
[49] E. Le Ferrec, C. Chesne, P. Artusson, D. Brayden, G. Fabre, P. Gires, F. Guillou, M. Rousset, W. Rubas, M.L. Scarino, In vitro Models of the Intestinal Barrier. The Report and Recommendations of ECVAM Workshop 46, European Centre for the Validation of Alternative methods, Altern. Lab. Anim. ATLA, 2001649–668.
[50] J.E. Gonçalves, M. Ballerini Fernandes, C. Chiann, M.N. Gai, J. De Souza, S. Storpirtis, Effect of pH, mucin and bovine serum on rifampicin permeability through Caco-2 cells, Biopharm. Drug Dispos. 33 (2012) 316–323, https://doi.org/10.1002/bdd.1802.
[51] W. Wu, C. Gaucher, R. Diab, I. Fries, Y.-L. Xiao, X.-M. Hu, P. Maincent, A. Sapin-Minet, Time lasting S-nitrosoglutathione polymeric nanoparticles delay cellular protein S-nitrosation, Eur. J. Pharm. Biopharm. Off. J. Arbeitsgemeinschaft Pharm. Verfahrenstechnik EV 89 (2015) 1–8, https://doi.org/10.1016/j.ejpb.2014.11.005.
[52] W. Wu, C. Gaucher, I. Fries, X.-M. Hu, P. Maincent, A. Sapin-Minet, Polymer nanocomposite particles of S-nitrosoglutathione: a suitable formulation for protection and sustained oral delivery, Int. J. Pharm. 495 (2015) 354–361, https://doi.org/10.1016/j.ijpharm.2015.08.074.
[53] K.U. Shah, S.U. Shah, N. Dilawar, G.M. Khan, S. Gibaud, Thiomers and their potential applications in drug delivery, Expert Opin. Drug Deliv. 14 (2017) 601–610, https://doi.org/10.1080/17425247.2016.1227787.

UNCORRECTED PROOF